

THE EFFECTS OF GALAXY INTERACTIONS ON STAR FORMATION AND MORPHOLOGY

SABRINA HURLOCK¹, BEVERLY J. SMITH, AND MARK HANCOCK

Department of Physics, Astronomy, and Geology, East Tennessee State University, Johnson City, TN 37614

ABSTRACT

We analyze SARA (Southeastern Association for Research in Astronomy) optical images of twelve interacting galaxy systems selected from the Arp Atlas, and compare with GALEX (Galaxy Evolution Explorer) UV images and with Spitzer infrared ($3.6\ \mu\text{m}$ and $8.0\ \mu\text{m}$) images. Using SARA, we observe the galaxies in visible wavelengths including B, V, and R broadband filters and narrowband redshifted $H\alpha$ filters. By analysing these images, we are able to determine the effects that interaction has on the structure of the galaxy including the formation of bridges and tails, and where new star formation is occurring.

Subject headings: galaxies: interactions — galaxies: starburst

1. INTRODUCTION

Since the first publication of Arp's Atlas of Peculiar Galaxies (1966), both professional and amateur astronomers have been fascinated with interacting galaxies. These discoveries have sparked a wave of research in trying to understand exactly what happens when these massive objects collide with or pass very close to each other (see review by Struck 1999). Since then, astronomers have studied the extreme morphological effects that interaction has on the structure of the galaxy and the accelerated and prolonged rates of star formation. The most prominent features in interacting galaxy systems are the tidal features. When a galaxy passes in close proximity to another galaxy, gravitational forces cause stars and interstellar gas and dust to form bridges between the two galaxies and/or form tails (Toomre & Toomre 1972). These interactions can also drastically alter the overall shape and structure of the galaxy; galaxies can merge into one enormous elliptical/lenticular galaxy, the galaxies can become elongated, or spiral galaxies can have their arms ripped away. When matter from a merging galaxy falls into or passes near its companion, the infalling matter interacts with material from the other galaxy, which can result in a boom in star formation. Evidence for this comes with analyzing $H\alpha$ images of galaxy collisions where clumps of star formation are observed in both the galactic disks and in areas such as the tails. These results are confirmed by comparing optical images with GALEX UV images and by using the Spitzer infrared images.

2. OPTICAL OBSERVATIONS

The galaxies in our sample are listed in Table 1 while the details of the observations are given in Table 2. Optical observations of these galaxies were made using the Southeastern Association for Research in Astronomy (SARA) 0.9 meter telescope with the Axiom/Apogee 2048x2048 CCD (U42) and also with the Apogee Alta 1024x1024 CCD (U55) camera. Multiple ten minute exposures were taken of each galaxy in several different wavelengths including broadband B, V, and R filters, and narrowband (bandwidth 7nm) redshifted $H\alpha$ filters centered at 659, 664, or 671 nm. We also obtained twilight-sky flat fields and observed standard stars. We encountered a few problems while observing such as autoguider malfunctions, tracking problems, and ghost images.

3. DATA REDUCTION

We used the Image Reduction and Analysis Facility (IRAF) program to remove the bias and dark current from the images, flat-field the data, align the images, and combine the images. In order to obtain a pure $H\alpha$ image, we must first subtract out the continuum, or starlight, using the R band image. These continuum subtractions allow us to view areas of intense star formation ($H\text{ II}$ regions) that we would otherwise not be able to distinguish due to the intensity of the starlight. Before continuum-subtraction, the R band was convolved to match the point-spread function of the $H\alpha$ image using the IRAF routine "psfmatch". When there is a gradient in the images, usually caused by either the moon or a very bright star in the field, we use the IRAF routine "imsurfitt" to remove the gradient.

4. ULTRAVIOLET AND INFRARED OBSERVATIONS

We compare the SARA data with images of broadband far and near-ultraviolet filters centered at $1550\ \text{\AA}$ and $2275\ \text{\AA}$ respectively, taken with the Galaxy Evolution Explorer (GALEX) space telescope. GALEX is a 0.6 meter NASA telescope that was launched on April 28, 2003 from Cape Canaveral in Florida. The GALEX images have been presented by Giroux et al. (2006), Hancock et al. (2007), and Giroux et al. (2008).

We also compared with the Spitzer Space Telescope $3.6\ \mu\text{m}$ and $8.0\ \mu\text{m}$ broadband images. Spitzer is a NASA 0.85 meter telescope which was launched on August 25, 2003 from Cape Canaveral in Florida. The Spitzer images have previously been published by Smith et al. (2007).

5. ANALYSIS

Our data revealed many exciting tidal features and interesting areas of star formation. In this section we discuss each galaxy system in turn.

Arp 65 (NGC 90/93, Figure 1): NGC 93 (eastern galaxy) is classified as an Sab galaxy, meaning it is a spiral galaxy with tightly wound arms and a large galactic bulge. There is no observable bridge between this galaxy and its companion. In the continuum-subtracted $H\alpha$ images, we found that the $H\text{ II}$ regions are concentrated at the center of the galaxy. NGC 90 is categorized as an SABc because it is a barred spiral galaxy with very open arms and a small galactic bulge. This galaxy has long tails extending to the northwest and southeast of the galactic bulge. $H\text{ II}$ regions are observed in the

Electronic address: sabrinahurlock@hotmail.com; smithbj@etsu.edu; hancockm@etsu.edu

TABLE 1
Interacting Galaxies Observed with SARA

System Name	Other Names	RA (J2000) ¹	DEC ¹	Distance ¹ (Mpc)	Type ¹
Arp 65	NGC 90/93	00h 21m 51.4s	+22d 24m 00s	70	SABc/Sab
Arp 82	NGC 2535/2536	08h 11m 14.7s	+25d 11m 36s	60	Sc/SBc
Arp 86	NGC 7752/7753	23h 47m 01.6s	+29d 28m 17s	63	SO/SABb
Arp 101	UGC 10164/10169	16h 04m 30.0s	+14d 48m 01s	66	E-SO/SO
Arp 120	NGC 4435/4438	12h 27m 43.0s	+13d 02m 38s	16	SO/SA
Arp 205	NGC 3448/UGC 6016	10h 54m 39.2s	+54d 18m 19s	21	SO-a/IAB
Arp 261	MGC 2-38-16	14h 49m 32.7s	-10d 09m 47s	29	E?
Arp 283	NGC 2798/2799	09h 17m 26.9s	+41d 59m 48s	28	SBa/SBd
Arp 285	NGC 2854/2856	09h 24m 09.6s	+49d 13m 34s	33	SBb/Sc
Arp 290	IC 195/196	02h 03m 47.1s	+14d 43m 26s	45	SO/SB
Arp 305	NGC 4016/4017	11h 58m 37.3s	+27d 29m 27s	52	Sd/Sbc
NGC 4194	NGC 4194	12h 14m 09.5s	+54d 31m 37s	37	IB

¹ Obtained from the NASA/IPAC Extragalactic Database (NED)

TABLE 2
Dates/Conditions of Observation

System Name	Date Observed	CCD ²	Filter	Images X Exposure Time	Weather Conditions
Arp 65	10/9/05	U55	R	4 x 600 seconds	Clear
—	—	U55	671	3 x 600 seconds	Clear
Arp 65	10/11/05	U55	R	3 x 600 seconds	Clear
—	—	U55	671	3 x 600 seconds	Clear
Arp 65	11/21/06	U42	R	3 x 600 seconds	Clear
—	—	U42	671	4 x 600 seconds	Clear
Arp 65	11/22/06	U42	B	4 x 600 seconds	Clear
—	—	U42	V	3 x 600 seconds	Clear
Arp 82	12/1/05	U55	B	3 x 600 seconds	Clear
Arp 82	1/16/07	U42	B	5 x 600 seconds	Clear
Arp 82	2/15/07	U42	V	3 x 600 seconds	Clear
Arp 86	12/1/05	U55	B	3 x 600 seconds	Clear
Arp 101	5/25/06	U55	R	5 x 600 seconds	Clear
—	—	U55	664	7 x 600 seconds	Clear
Arp 120	1/16/07	U42	R	4 x 600 seconds	Clear
—	—	U42	659	6 x 600 seconds	Clear
Arp 205	2/15/07	U42	R	4 x 600 seconds	Clear
—	—	U42	659	6 x 600 seconds	Clear
Arp 261	2/15/07	U42	R	3 x 600 seconds	Clear
—	—	U42	659	3 x 600 seconds	Clear
Arp 283	1/16/07	U42	R	4 x 600 seconds	Clear
—	—	U42	659	5 x 600 seconds	Clear
Arp 285	1/29/06	U55	R	3 x 600 seconds	Cloudy
—	—	U55	664	7 x 600 seconds	Cloudy
Arp 290	10/9/05	U55	R	4 x 600 seconds	Clear
—	—	U55	664	3 x 600 seconds	Clear
Arp 290	10/11/05	U55	R	3 x 600 seconds	Clear
—	—	U55	664	3 x 600 seconds	Clear
Arp 305	2/16/07	U42	R	4 x 600 seconds	Clear
—	—	U42	664	5 x 600 seconds	Clear
NGC 4194	3/15/07	U42	R	3 x 600 seconds	Clear
—	—	U42	664	5 x 600 seconds	Clear

² U42: Axiom/Apogee 2048x2048; U55: Apogee/Alta 1024x1024.

nucleus, faintly in some places in the arms, and in one particularly bright clump in the northern tail. The clump in the northern tail was confirmed by comparison with 8.0 μm images obtained by the Spitzer Space Telescope.

Arp 82 (NGC 2535/2536, Figure 2): Arp 82 is a very exciting system to study because of the prominent tidal features

and several areas of star formation. NGC 2536 is the southern galaxy and is categorized as an SBc galaxy. Star formation is strongest in the center of the galaxy and the most noticeable tidal feature is that of a bridge connecting to its companion NGC 2535.

NGC 2535 is the northern galaxy of the pair and is classi-

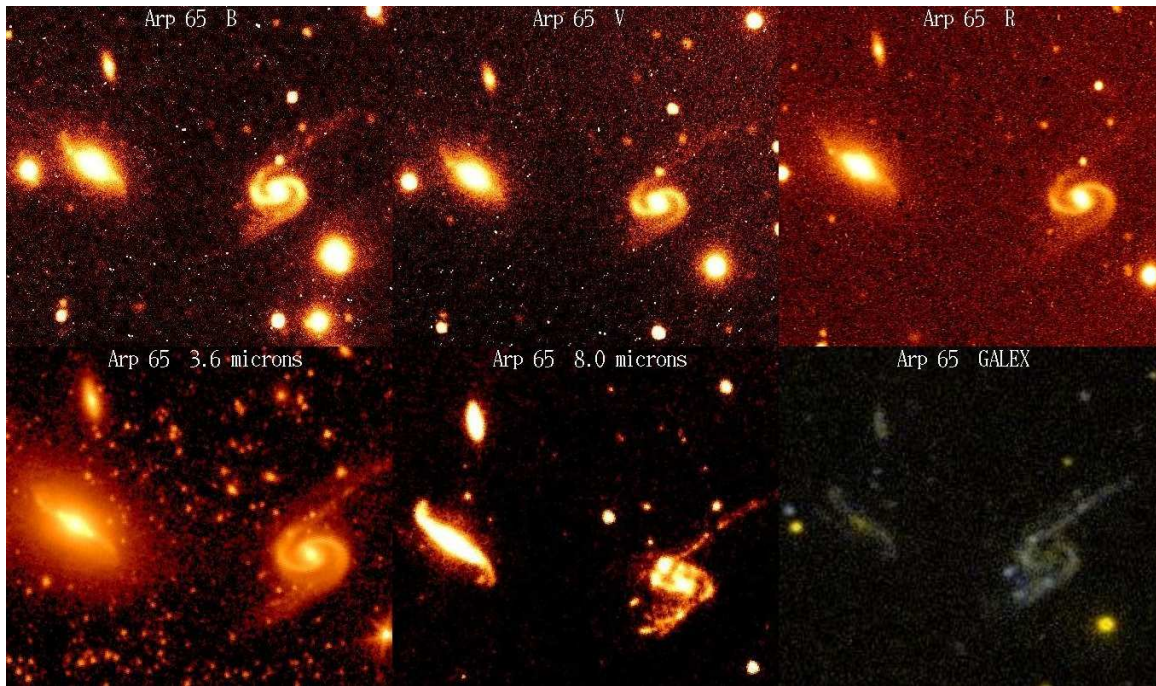


FIG. 1.— North is up and east is left. From left to right: Arp 65 filters B, V, R, 3.6 μm , 8.0 μm , and GALEX (FUV is blue and NUV is yellow).

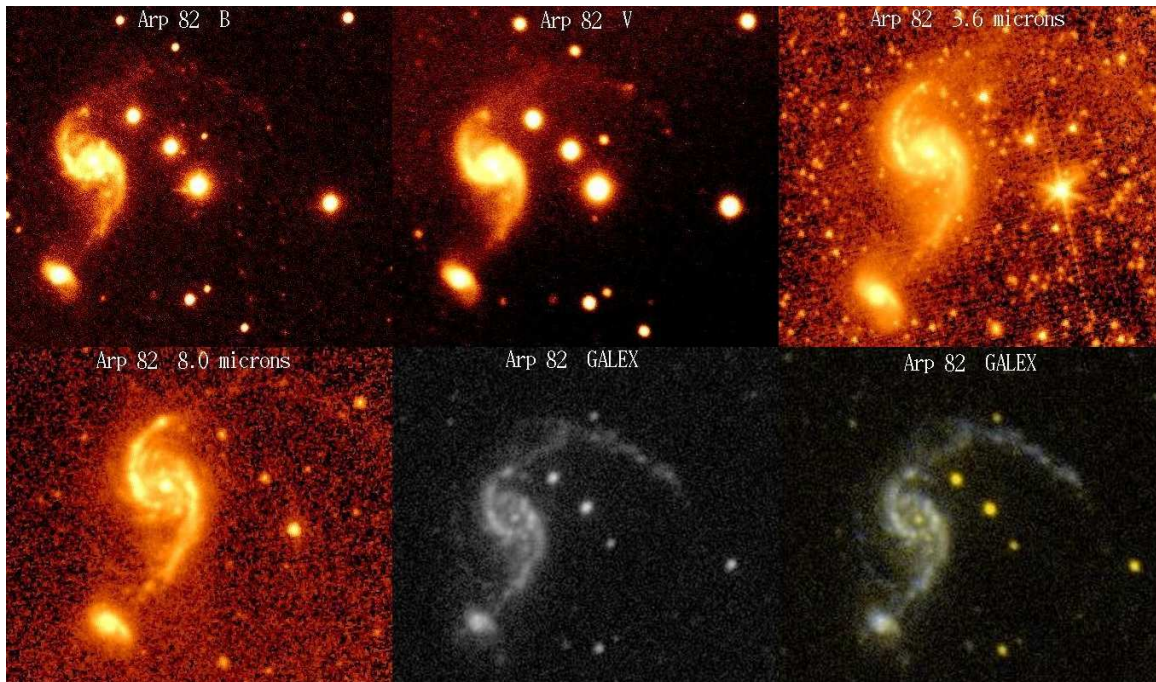


FIG. 2.— North is up and east is left. From left to right: Arp 82 filters B, V, 3.6 μm , 8.0 μm , GALEX (NUV only), and GALEX (FUV is blue and NUV is yellow).

ified as an Sc spiral galaxy due to the openness of its arms. In addition to the bridge, NGC 2536 has a magnificent tail that extends far to the western side of the galaxy. In addition, NGC 2536 has two secondary arcs, one extending east from the bridge to the south of the galactic disk and the other extending to the west north of the galactic disk. These arcs are thought to have been formed from a previous interaction. This feature is best viewed in the GALEX UV image but is also visible in the B and V filters. From the optical filters that we used (B and V), the tidal features are best viewed using the

V filter, whereas the clumps of star formation are more easily seen with the B filter. A detailed GALEX/Spitzer/SARA $\text{H}\alpha$ analysis of this system has already been completed (Hancock et al. 2007) which shows 26 clumps located within Arp 82, the brightest of which is located southwest of the galactic nucleus.

Arp 86 (NGC 7752/7753, Figure 3): Arp 86 is an M51-like system at a distance of 63 Mpc. NGC 7752, the smaller galaxy to the southwest, is classified as an SO galaxy (large galactic bulge but no spiral arms). The larger galaxy is clas-

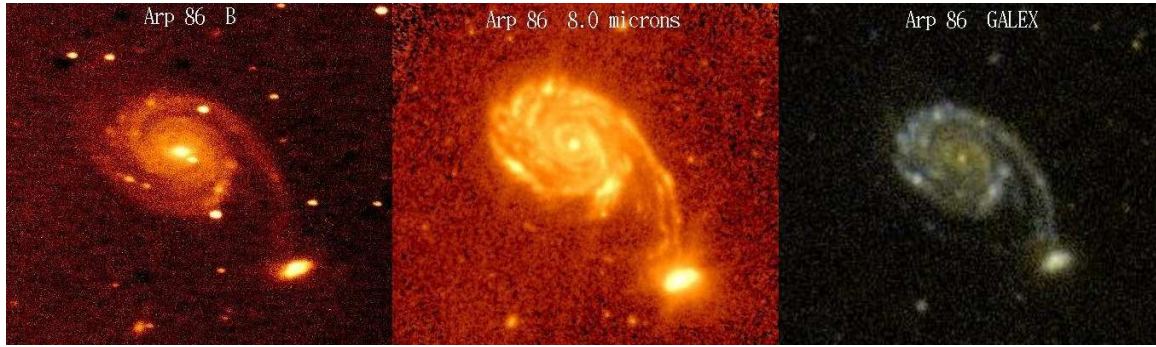


FIG. 3.— North is up and east is left. From left to right: Arp 86 filters B, 8.0 μm , and GALEX (FUV is blue and NUV is yellow). Note the tracking problems in the B image.

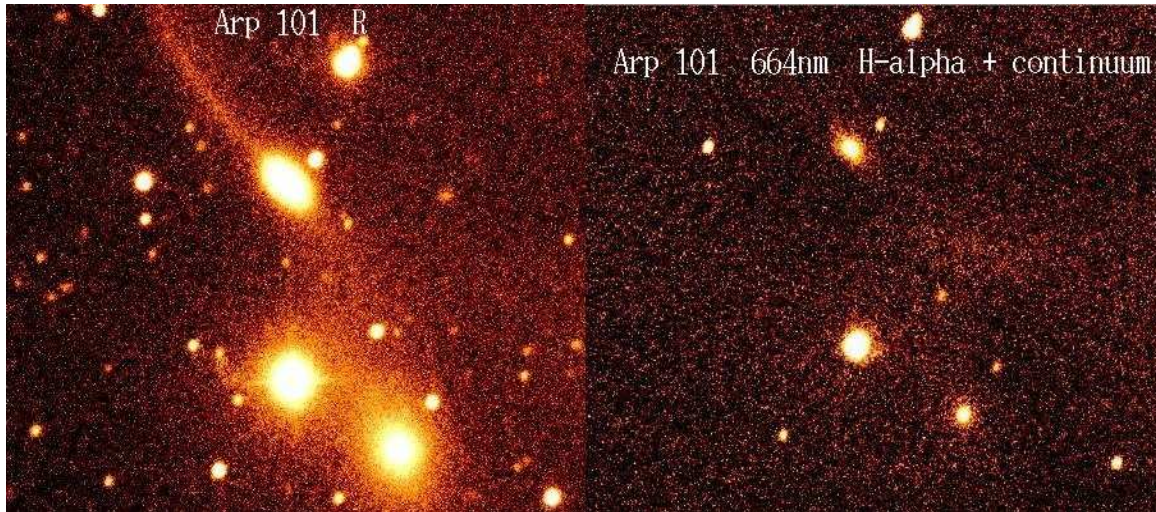


FIG. 4.— North is up and east is left. From left to right: Arp 101 filters R, and 664 nm.



FIG. 5.— North is up and east is left. From left to right: Arp 120 filters R, Smoothed continuum-subtracted $\text{H}\alpha$, and GALEX (FUV is blue and NUV is yellow).

sified as an SABC galaxy due to the small size of the galactic bulge and its open spiral arms. The most obvious tidal feature is that of the bridge connecting the two companions together. NGC 7753 has several small clumps of star formation encircling the nucleus.

Unfortunately, on this night we had tracking problems with SARA which resulted in our images being severely elongated. However, when we compared the SARA images with Spitzer and GALEX images, we found that the clumps observed in the optical wavelengths coincided with clumps observed in the infrared and ultraviolet.

Arp 101 (UGC10164/10169, Figure 4): Arp 101 is the result of an interaction between UGC 10164 and UGC 10169.

UGC 10164 is located south of UGC 10169 and is a beautiful example of an elliptical galaxy. UGC 10169 is the northern galaxy of the pair and is classified as an SO galaxy. The only visible tidal features are a magnificent tail on UGC 10169 extending to the northeast and a great deal of interstellar gas and dust in a bridge between the two galaxies.

Arp 120 (NGC 4435/4438, Figure 5): Arp 120 is the result of a head-on collision between NGC 4435 (north) and NGC 4438 (south). NGC 4435/4438 are categorized as SO/SA galaxies respectively. The morphological features of these galaxies are different than many interacting systems in that there is not one notable bridge connecting the two together, rather the space between the two galaxies is filled with a sub-

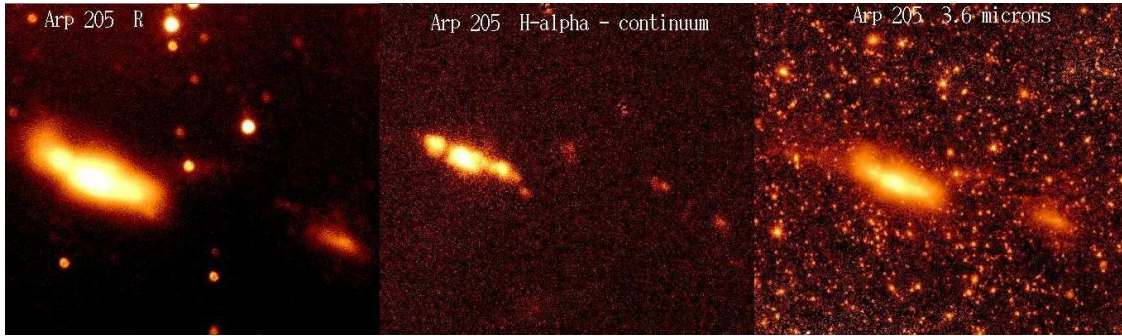


FIG. 6.— North is up and east is left. From left to right: Arp 205 filters R, Continuum-subtracted H α , and 3.6 μ m.

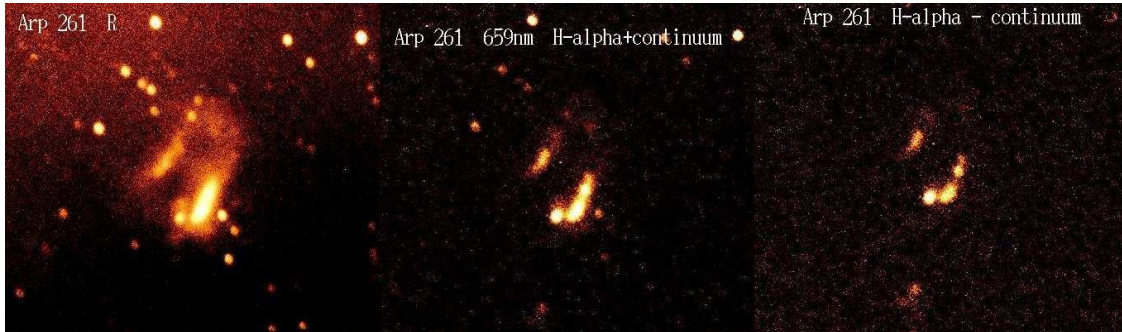


FIG. 7.— North is up and east is left. From left to right: Arp 261 filters R, 659 nm, and Continuum-subtracted H α .

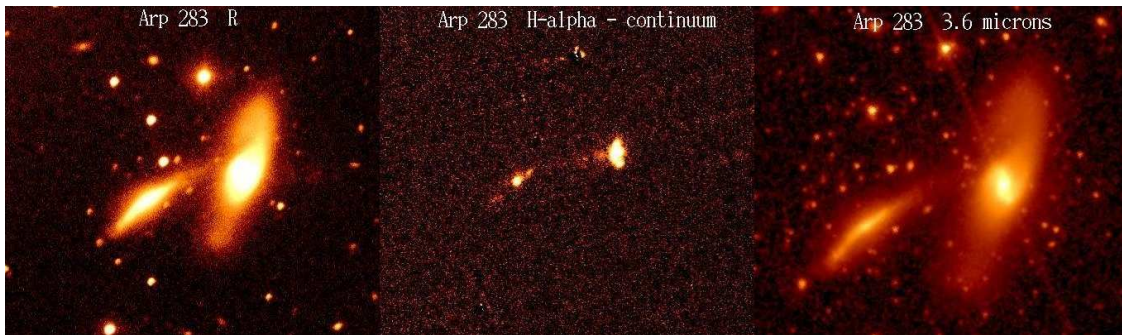


FIG. 8.— North is up and east is left. From left to right: Arp 283 filters R, Continuum-subtracted H α , and 3.6 μ m.

stantial amount of interstellar gas and dust. This was likely caused when NGC 4435 passed through NGC 4438. NGC 4438 also displays magnificent dust lanes on the western edge of the galactic bulge and small arms extending from the nucleus. After analyzing the H α images, we found that H II regions were found around the nucleus of both galaxies, with the most star formation taking place in NGC 4438. Filaments of H α are also seen extending from the nucleus of NGC 4438. This system has been extensively studied by Kenney et al. (1995).

Arp 205 (NGC 3448/UGC 6016, Figure 6): UGC 6016 is the smallest of the two companions and is classified as an irregular galaxy. This galaxy was barely visible in our R band optical images, but we found a small H II region that was detected in the nuclear area. There were no observed tidal features due to the faintness of the galaxy. NGC 3448, an SO galaxy, has some very note-worthy features. There appears to be a sort of dusty halo surrounding the galaxy and a small concentration of dust and gas located southwest to the plane of the galaxy. The continuum-subtracted H α images also revealed

three intense areas of star formation which were also visible in the Spitzer 8.0 μ m images. The largest area of star formation is located in the center of the galaxy while two slightly smaller clumps are located to the east and west sides of the center respectively.

Arp 261 (MGC 2-38-16, Figure 7): Similar to Arp 120, Arp 261 is likely the result of a head-on collision which is the reason for the peculiar shapes of both galaxies. The most obvious morphological feature is that of a large amount of interstellar gas and dust located between the two galaxies. The northern galaxy is very faint in the R band filter, however there seems to be a significant amount of H α emission originating from the center of the galaxy. The southern galaxy has three major areas of star formation that are similar in structure to NGC 3448 in Arp 205 in that the most concentrated area of star formation is coming from the area around the center of the galaxy with two somewhat smaller clumps on the eastern and northwestern sides of the nucleus.

Arp 283 (NGC 2798/2799, Figure 8): Arp 283 consists of NGC 2798/2799, classified as SBa/SBd types respectively.

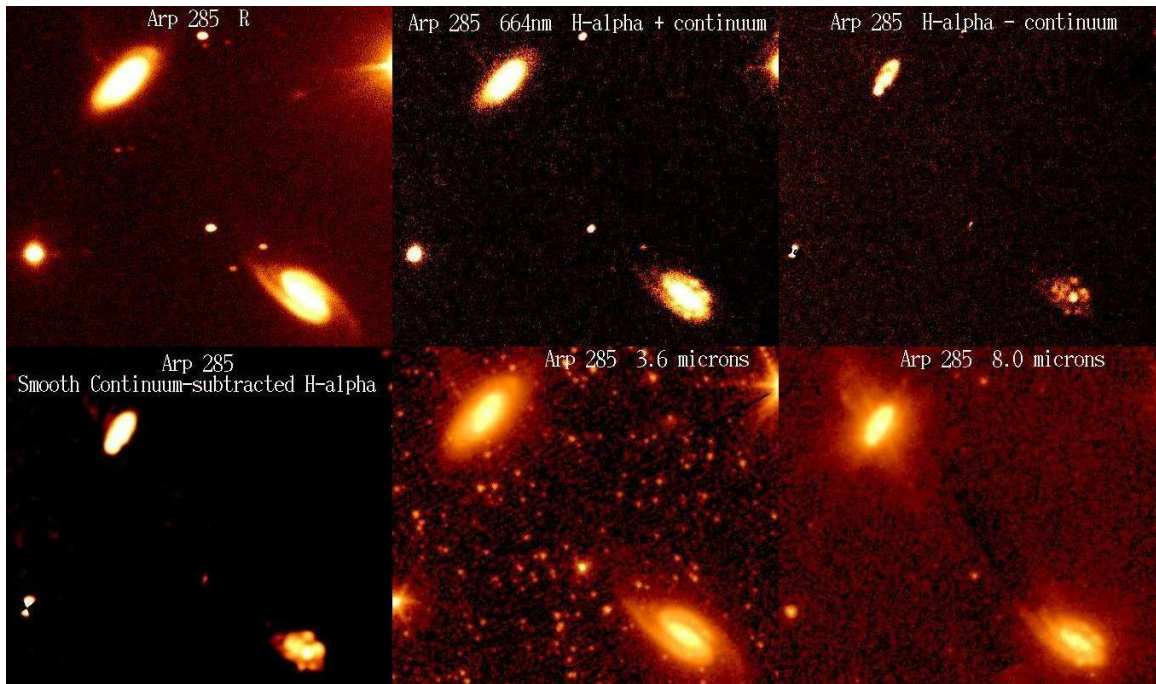


FIG. 9.— North is up and east is left. From left to right: Arp 285 filters R, 664 nm, Continuum-subtracted H α , Smoothed continuum-subtracted H α , 3.6 μ m, and 8.0 μ m.

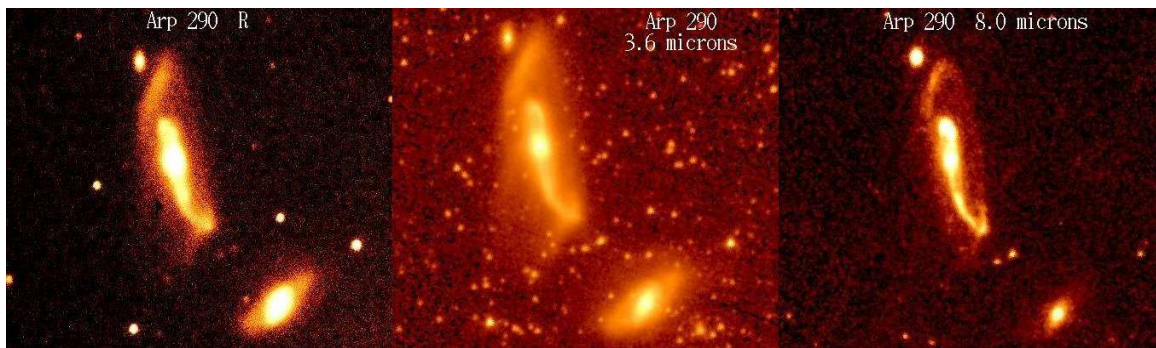


FIG. 10.— North is up and east is left. From left to right: Arp 290 filters R, 3.6 μ m, and 8.0 μ m.

NGC 2799 (east) is a saucer-shaped galaxy that is in the process of colliding with NGC 2798. The most apparent morphological feature is the bridge extending northwest of the nucleus. H II regions are detected at the center of the galaxy and in a small clump located to the northwest of the galactic center. NGC 2798 also has some interesting tidal features, the most obvious of which is its spiral arms. The southern arm appears to have most of its components stripped away, leaving only sparse areas of dust and gas. H α images show that there is no star formation occurring in these regions. H II regions are detected in the nucleus of the galaxy as well as in the bridge in clumps spanning the distance between the galaxies.

Arp 285 (NGC 2854/2856, Figure 9): NGC 2854/2856 are categorized as SBb and Sc type galaxies respectively and the system is located at a distance of 32.5 Mpc. NGC 2854 (south) has a bridge connecting it to NGC 2856 and an opposing tail extending to the southwest. Analysis of H α images revealed regions of star formation in the nucleus and in several clumps encircling the nucleus. The clumps around the nucleus were also detected in the 8.0 μ m Spitzer image. The most conspicuous tidal feature of NGC 2856 is that of a tail which points to the north. There is also one clump of star

formation located in this tail which GALEX and Spitzer data both confirmed. Star formation is distributed throughout the galactic disk with the largest area located in the center with two other circular areas located on the eastern and western sides respectively; this is referred to as “beads on a string” star formation. A detailed analysis of these images of Arp 285 is presented in Smith et al. (2008).

Arp 290 (IC 195/196, Figure 10): Arp 290 is the aftermath of a collision between IC 195 (southern, lenticular galaxy) and IC 196 (northern, SB type galaxy). H α imaging of IC 195 shows that the most H α emission is coming from the central region. IC 196 has striking morphological features such as a dusty “halo” surrounding the galaxy which is visible in both the optical and infrared wavelengths. Review of the H α images show that there is emission occurring in the galactic disk as well as in the nucleus.

Arp 305 (NGC 4016/4017, Figure 11): Arp 305 is the result of an interaction between NGC 4016 and NGC 4017 which are designated as Sd and Sbc galaxies respectively. NGC 4017 is the southern galaxy and exhibits a bridge extending northwest toward NGC 4016 and an opposing tail pointing northeast. H α images show us that there is star formation occurring

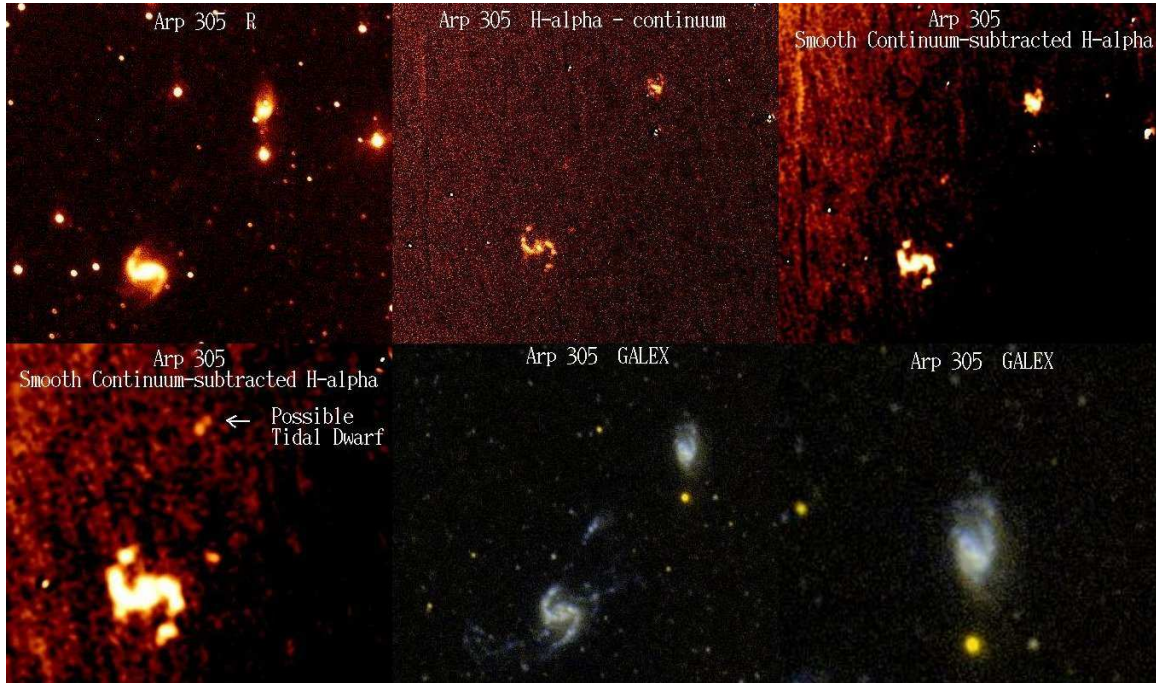


FIG. 11.— North is up and east is left. Row 1 from left to right: Arp 305 filters R, Continuum-subtracted $H\alpha$, and Smoothed continuum-subtracted $H\alpha$. Row 2 from left to right: Zoomed-in view of the southern galaxy NGC 4017 in smoothed $H\alpha$, GALEX (FUV is blue and NUV is yellow), and a GALEX image of a zoomed-in view of the northern galaxy NGC 4016.

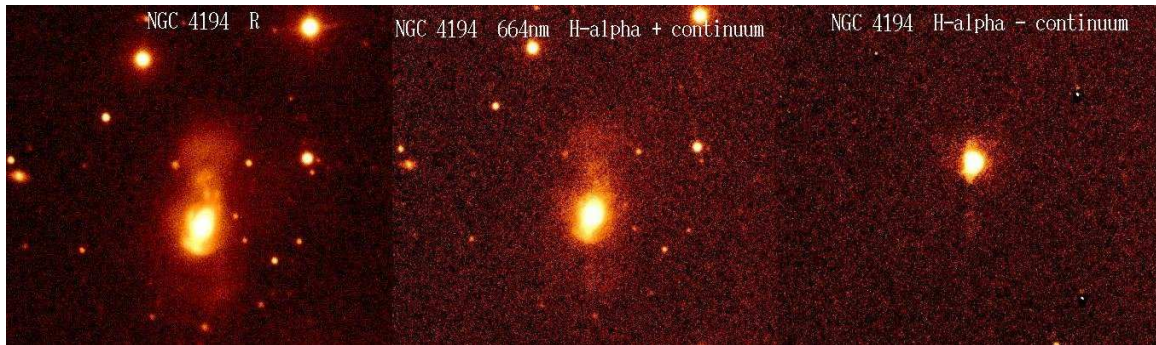


FIG. 12.— North is up and east is left. From left to right: NGC 4194 filters R, 664 nm, and continuum-subtracted $H\alpha$.

in clumps along both arms and possibly in the nucleus as well. There is also a small $H\text{ II}$ region located between the galaxies, in what appears to be a bridge connecting the objects together. This formation is also detected in the GALEX UV image.

The morphological features of NGC 4016 include a somewhat misshapen bulge with a dusty disk surrounding the galaxy. $H\alpha$ emission was detected in the galactic bulge and also in small clusters along the spiral arms. Another $H\text{ II}$ region was detected in the bulge coming off of the galactic nucleus extending to the southwest. There is also a “figure-eight” formation that is located to the northeast and southwest of the main galactic disk. How this feature was formed has only been speculated; it is possible that it was formed from a previous interaction or by accretion of material from its companion galaxy. This system is discussed in detail in Hancock et al. (2008).

NGC 4194 (Medusa, Figure 12): This is an object where the two galaxies have already merged together to form one enormous peculiar galaxy. The remnants of tidal features include an extremely dusty, pendulum-shaped formation extending far to the north of the main portion of the galaxy and a smaller

similar feature to the south. The pendulum feature is visible in the narrow band 664 nm filter in addition to the visible R band. There are also three arm-like features, two of which extend northward and the other to the east of the galactic center. Star formation appears to be concentrated in the center of the galaxy.

6. SUMMARY AND CONCLUSIONS

To further understand the effects of galactic interactions, we have observed twelve interacting galaxy samples with the SARA telescope. Using the broadband R, B, and V filters and multiple narrowband $H\alpha$ filters, we are able to determine the size and location of $H\text{ II}$ regions and observe the changes in the structures of the galaxy. In this sample, we observed some systems having unusual morphological features and interesting areas of star formation. First, we found that Arp 82 has a set of secondary arcs, one to the north of disk pointing west and the second to the south of the disk pointing east. These arcs were possibly formed by a previous interaction. Second, in Arp 283 we detected clumps of $H\text{ II}$ emission in the bridge connecting the two galaxies. Finally, there were two features in Arp 305 that were noteworthy. First, there appears

to have been a tidal dwarf galaxy formed by the interaction of NGC 4016 and NGC 4017. Secondly, in NGC 4016 (northern galaxy of Arp 305) there is a “figure-eight” feature that is oriented to the northeast and southwest of the galactic center. Our results were confirmed by comparison with data obtained from GALEX UV images and Spitzer infrared images.

This research was made possible by the NASA LTSA grant NAG5-13079. We thank the Spitzer and GALEX teams for

their contributions to this project. We thank Curt Struck, Mark Giroux, Phil Appleton, Vassilis Charmandaris, and Bill Reach for help in acquiring the Spitzer and GALEX data. This research has made use of the NASA/IPAC Extragalactic Database (NED) that is operated by the Jet Propulsion Laboratory at the California Institute of Technology, which is under contract with the National Aeronautics and Space Administration.

REFERENCES

- Arp, H. 1966, *Atlas of Peculiar Galaxies* (Pasadena: Caltech)
- Giroux, M. L., Smith, B. J., Struck, C., Appleton, P. N., Charmandaris, V. 2005, *BAAS*, 37, 449
- Giroux, M. L., et al. 2008, in preparation.
- Hancock, M., Smith, B. J., Struck, C., Giroux, M. L., Appleton, P. N., Charmandaris, V., & Reach, W. T. 2007, *AJ*, 133, 676
- Hancock, M., et al. 2008, in preparation.
- Kennedy, J. D. P., Rubin, V. C., Planesas, P., and Young, J. S. 1995, *ApJ*, 438, 135
- Smith, B. J., et al. 2007, *AJ*, 133, 791
- Smith, B. J., et al. 2008, *AJ*, submitted.
- Struck, C., 1999, *Phys. Rep.*, 321, 1
- Toomre, A., & Toomre, J. 1972, *ApJ*, 178, 623